

Research Article

# A quantitative model for mRNA translation in *Saccharomyces cerevisiae*

Tao You<sup>1</sup>, George M Coghill<sup>2</sup> and Alistair J. P. Brown<sup>3\*</sup>

<sup>1</sup>Physics Department, School of Natural and Computing Sciences, University of Aberdeen, UK

<sup>2</sup>Computing Science Department, School of Natural and Computing Sciences, University of Aberdeen, UK

<sup>3</sup>Institute of Medical Sciences, School of Medical Sciences, University of Aberdeen, UK

\*Correspondence to:

Alistair J. P. Brown, School of Medical Sciences, University of Aberdeen, Institute of Medical Sciences, Foresterhill, Aberdeen AB25 3ZD, UK.

E-mail: al.brown@abdn.ac.uk

## Abstract

**Messenger RNA (mRNA) translation is an essential step in eukaryotic gene expression that contributes to the regulation of this process. We describe a deterministic model based on ordinary differential equations that describe mRNA translation in *Saccharomyces cerevisiae*. This model, which was parameterized using published data, was developed to examine the kinetic behaviour of translation initiation factors in response to amino acid availability. The model predicts that the abundance of the eIF1–eIF3–eIF5 complex increases under amino acid starvation conditions, suggesting a possible auxiliary role for these factors in modulating translation initiation in addition to the known mechanisms involving eIF2. Our analyses of the robustness of the mRNA translation model suggest that individual cells within a randomly generated population are sensitive to external perturbations (such as changes in amino acid availability) through Gcn2 signalling. However, the model predicts that individual cells exhibit robustness against internal perturbations (such as changes in the abundance of translation initiation factors and kinetic parameters). Gcn2 appears to enhance this robustness within the system. These findings suggest a trade-off between the robustness and performance of this biological network. The model also predicts that individual cells exhibit considerable heterogeneity with respect to their absolute translation rates, due to random internal perturbations. Therefore, averaging the kinetic behaviour of cell populations probably obscures the dynamic robustness of individual cells. This highlights the importance of single-cell measurements for evaluating network properties. Copyright © 2010 John Wiley & Sons, Ltd.**

**Keywords:** mRNA translation; robustness; eukaryotic translation initiation; kinetic model

Received: 8 December 2009

Accepted: 13 February 2010

## Introduction

Translation is the process by which the coding sequence of a particular messenger RNA (mRNA; in nucleotides) is translated into a specific protein (the corresponding amino acid sequence) via a specific molecular machine (the ribosome). As such, mRNA translation is an essential step in gene expression for all organisms. Furthermore, the rate at which genes are expressed is partly determined

by the rate of mRNA translation, and regulation at the level of mRNA translation contributes significantly to the expression of certain genes in all organisms. Indeed, it has been suggested that changes in mRNA transcript levels account for only 20–40% of the variations seen at the level of the proteome (Brockmann *et al.*, 2007). Specific examples of translational regulation in yeast include the *GCN4*, *CPA1* and *YAP1* mRNAs (Delbecq *et al.*, 1994; Vilela *et al.*, 1998; Hinnebusch, 2005).

mRNA translation is divisible into three main steps. During translation initiation in eukaryotic cells, a functional ribosome assembles at the start of an mRNA coding region in a complex series of reactions involving as many as 11 eukaryotic initiation factors (eIFs; Kapp and Lorsch, 2004). This is followed by translation elongation, during which amino acids are delivered to the ribosome on cognate transfer RNAs (tRNAs) and then covalently attached to the growing polypeptide chain as the ribosome translocates from codon to codon on the mRNA. When the ribosome encounters a stop codon, translation is terminated, the ribosome dissociates from mRNA and the new protein molecule is released.

mRNA initiation, elongation and termination are connected sequentially in a temporal order. Hence, the slowest step must largely determine the rate of the entire process under steady-state conditions. mRNA translation is primarily regulated at the level of initiation (Marintchev and Wagner, 2004), and this generalization is supported by recent studies of ribosomal density on mRNA molecules (Arava *et al.*, 2005; Ingolia *et al.*, 2009). Arava and co-workers reasoned that it should be possible to define the rate-limiting step in translation by mapping ribosome density across different parts of a specific mRNA. Ribosomes accumulate at regions of the slowest step. For example, ribosomes can congregate at regions containing clusters of non-preferred codons where translation elongation is relatively slow, thereby leading to a non-uniform ribosomal distribution along the mRNA. Also, ribosomes can queue at the end of an mRNA where termination is relatively slow (Arava *et al.*, 2005). Some mathematical models were developed to quantitatively explain these phenomena around three decades ago (Bergmann and Lodish, 1979; Harley *et al.*, 1981; Godefroy-Colburn and Thach, 1981). Arava and co-workers investigated several selected yeast mRNAs and found that they display uniform ribosome densities, indicating that, for most mRNAs, translation is limited at initiation (Arava *et al.*, 2005). A later genome-wide study exploiting deep sequencing technique found a general trend of elevated 5' ribosome density that is independent of mRNA length (Ingolia *et al.*, 2009). This is also in agreement with the idea that translation is limited at the initiation step. Therefore, defining the kinetics of translation initiation is central to an understanding of mRNA translation.

The development of a mathematical model encompassing translation initiation and amino acid metabolism is a useful goal because, although the initiation of mRNA translation has been studied intensively, the sheer complexity of this process can make it difficult to interpret experimental data in a unique way. As described by Marintchev and Wagner (2004), this can lead to inconsistent views about the properties of individual eIFs. A quantitative model could be used to test the validity of competing hypotheses. In addition, a model encompassing translation initiation apparatus could be used to predict the operational status of translation initiation factors under different amino acid availabilities, and the extent to which these factors might contribute to the regulation of mRNA translation. For example, *GCN4* is a master transcription factor that controls the expression of many amino acid biosynthesis genes. *GCN4* expression levels are primarily controlled at the translational level (Hinnebusch, 2005). Previous experiments on *GCN4* translation suggest that, in addition to eIF2, the translation of *GCN4* mRNA is also affected by an unknown factor, which might be eIF5 (Grant *et al.*, 1994). Using this model, we have been able to examine the behaviour of eIF5 under amino acid starvation conditions, and hence test this hypothesis.

Several mathematical models have been developed to explain the kinetics of translation initiation. For instance, the impact of each initiation factor upon translation was evaluated using flux control coefficients (Dimelow and Wilkinson, 2009). In addition, an ordinary differential equation (ODE) system that included all three steps of translation was proposed to investigate regulatory mechanisms in mRNA translation (Skjøndal-Bar and Morris, 2007). However, the former model did not relate translation initiation to amino acid metabolism, whereas the latter did not include initiation factors that are relevant to *GCN4* mRNA translation (i.e. eIF1, eIF3 and eIF5). Therefore, we have developed a mathematical model of translation initiation that is applicable to *GCN4* regulation during amino acid starvation.

Quantitative models can also be used to examine the emergent properties of complex biochemical networks, a challenge that is difficult to address without a computational framework. One such property is the robustness of living systems, whereby the functionality of biological networks

can persist in the face of internal and external perturbations (Kitano, 2007). mRNA translation is a fundamental process that is conserved in all species, and it has been investigated intensively. However, few have attempted to characterize the robustness of this process (Sangthong *et al.*, 2007). Therefore, in this study we have taken the first steps towards this goal by developing a deterministic model of eukaryotic translation initiation and exploring its properties.

## Materials and methods

### Mathematical modelling

The model of mRNA translation is a deterministic system of ordinary differential equations, which uses Michaelis–Menten kinetics to describe aminoacylation of histidine tRNA ( $v_3$ ,  $v_4$ ) and applies mass action kinetics to the other reactions. The equations and the parameterization are described in detail in the Supporting information. The model is available in SBML format in the BioModels Database (MODEL8459127548). The model was implemented in MATLAB<sup>®</sup> R2007a (The MathWorks Inc.) and solved using its built-in solver 'ode15s'.

Some kinetic parameters were taken from the literature or estimated on the basis of published experimental observations. The rest were optimized by an evolutionary computing algorithm implemented in C, with a population size of 200 for 300 generations (Runarsson and Yao, 2005). The actual runtime of the optimization on a desktop PC (Pentium 4 CPU, 3.0 GHz, 2.0 GHz RAM) was about 70 h. Published molecular binding affinities and kinetic parameter values obtained from *in vitro* assays were used to estimate possible ranges of the parametric space in which this optimization took place. After optimization, a sensitivity analysis of the model fitness with respect to each kinetic parameter (including those that are not optimization results) was carried out to evaluate which parameters cannot be estimated with reasonable accuracy by the experimental data. We have also analysed which reactions significantly affect the general mRNA translation rate ( $v_{34}$ ). Taken together, kinetic parameters that could not be constrained within reasonable limits were either estimated from the literature, or they did not have significant

impact on  $v_{34}$ . This strengthened confidence in the model. The parameterization and ensuing analyses are detailed in the Supporting information.

## Results

### The reaction network model

Our first step was the definition of the reaction network that underpins our understanding of translation initiation, based on the literature. In *S. cerevisiae*, translation initiation is regulated mainly through modulation of eIF2 or eIF4, which contribute to start codon recognition and the initial binding of mRNA by the ribosome, respectively (Figure 1). eIF2 is a G-protein: only the GTP-bound form is capable of binding Met-tRNA<sub>i</sub><sup>Met</sup> to form the ternary complex. This ternary complex (eIF2·GTP:Met-tRNA<sub>i</sub><sup>Met</sup>) is essential for translation initiation, interacting with the small 40S ribosomal subunit to form the 43S complex as a prelude to association with the mRNA. eIF2B is the guanine nucleotide exchange factor (GEF) that converts eIF2·GDP to its active eIF2·GTP form. Under stress conditions such as amino acid starvation, uncharged tRNAs accumulate in the cytoplasm, leading to activation of the eIF2 $\alpha$  kinase, Gcn2. Following its phosphorylation by Gcn2, eIF2 becomes a competitive inhibitor of eIF2B, thereby reducing GTP–GDP exchange on eIF2, causing translational activity to decrease (Hinnebusch, 2005). In addition to stress conditions, the uncharged tRNA level is also affected by tRNA charging activity, which is determined by amino acid transport and aminoacylation. Therefore, it is natural to include these individual biochemical reactions into this descriptive model, which ultimately aims to embody a comprehensive description of general amino acid control.

A second critical step that affects translation rates involves the initial association of the 40S ribosomal subunit with the mRNA molecule. eIF4E binds near the 5' end of the mRNA. It also can interact with poly-A binding protein (PABP), bound at the 3'-end of the mRNA, to create a circularized complex. eIF4E also associates with eIF3 via eIF4G, to promote loading of the ternary complex onto the mRNA. The accessibility of mRNA to eIF4E is controlled by 4E-binding protein (4E-BP), which in turn is controlled by the nutrient-sensing target

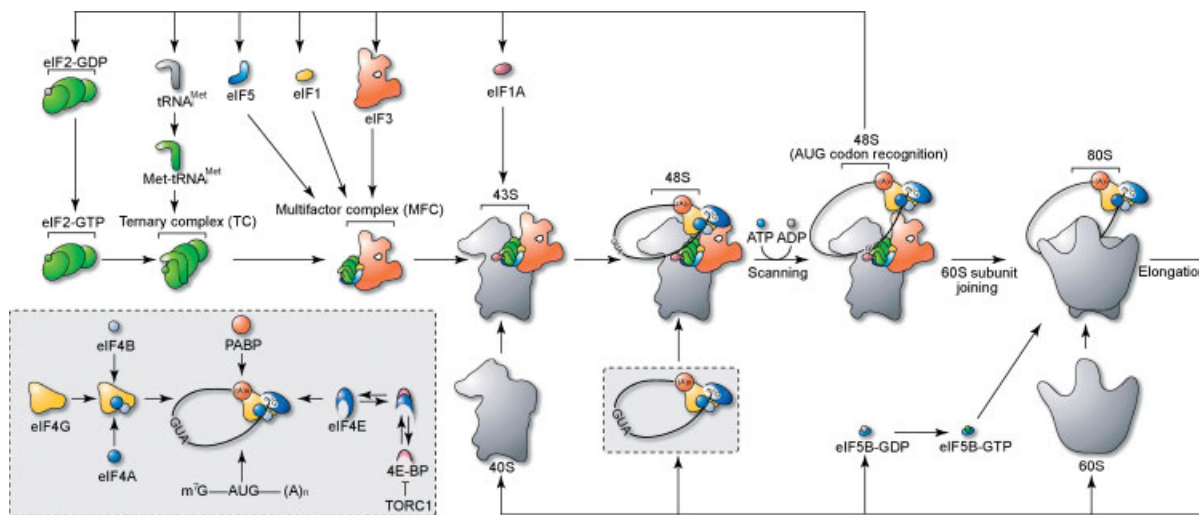


**Figure 1.** The process of translation initiation in eukaryotes. eIF2, which consists of three subunits ( $\alpha$ ,  $\beta$ ,  $\gamma$ ), binds translation initiator tRNA ( $\text{Met-tRNA}_i^{\text{Met}}$ ) and GTP to its  $\gamma$ -subunit to form the ternary complex (TC). TC subsequently binds to eIF3 via eIF5 to comprise the multifactor complex (MFC) that facilitates TC recruitment to the 40S ribosomal subunit. eIF4G is a scaffold protein that interacts with both eIF4E bound at the 5'-cap on the mRNA and the poly(A) tail binding protein (PABP), so that the translating mRNA can form a ring-like structure that favours translation re-initiation after translation termination. The scaffold protein eIF4G also has binding sites for the ATP-driven RNA helicase eIF4A and its co-factor eIF4B, both of which function together to remove the mRNA's secondary structure in the 5'-leader region to promote pre-initiation complex (PIC) assembly. Once an mRNA-loaded eIF4G binds to a 40S assembled with the necessary eIFs, the 40S starts to scan for the AUG triplet in an ATP-dependent fashion, facilitated by eIF4A and eIF4B. At the same time, eIF5 induces hydrolysis of the GTP in the TC, but the resultant GDP and phosphate is held by eIF1 until recognition of the AUG start codon. Once the  $\text{Met-tRNA}_i^{\text{Met}}$  is base-paired with the AUG codon in the P-site of the ribosome, the 40S subunit assumes a 'closed' conformation that is incompatible with further scanning and favours eIF1 dissociation. Release of eIF1 unblocks the phosphate. This triggers a subsequent release of the other eIF factors. The binding of eIF5B-GTP and its subsequent hydrolysis stimulates the joining of the large 60S ribosomal subunit

of rapamycin complex 1 (TORC1). TORC1 activity is downregulated by nitrogen starvation. This favours binding of 4E-BP to eIF4E, thereby limiting eIF4E access to mRNA and downregulating mRNA recruitment (Wullschleger *et al.*, 2006). In addition, TORC1 modulates Gcn2 activity via the Tap24-dependent phosphatase, Sit4/PP2A. When TORC1 is inhibited, for example in response to nitrogen starvation, Gcn2 is dephosphorylated at ser-577, thereby increasing its activity. This leads to a decrease in eIF2 activity (via the mechanisms described above) and to a decrease in mRNA translation (Cherkasova and Hinnebusch, 2003).

eIF2 activity is thought to be regulated by an additional mechanism. An eIF2-eIF5 complex has recently been implicated as a reservoir of eIF2 that modulates translational activity in response to nutritional status (Singh *et al.*, 2006). Overexpression of eIF5 is predicted to sequester eIF2, leading to downregulation of ternary complex formation in a *gcn2* $\Delta$  strain (Singh *et al.*, 2006).

The absolute levels of initiation factors in *S. cerevisiae* have been estimated (von der Haar and McCarthy, 2002; Ghaemmaghami *et al.*, 2003). Also, the levels of intermediate pre-initiation complexes have been measured in this yeast (Singh *et al.*, 2007). These studies provide important quantitative views of the operational status of the translational initiation apparatus *in vivo*. At the same time, a valuable thermodynamic framework has been established to describe interactions between eIFs and 40S *in vitro* (Algire *et al.*, 2002; von der Haar *et al.*, 2002; Maag *et al.*, 2003, 2005; Acker *et al.*, 2006; Passmore *et al.*, 2007). Efforts have also been made to define the kinetic mechanisms of eIF2B, although this has proved difficult (Rowlands *et al.*, 1988; Dholakia and Wahba, 1989; Nika *et al.*, 2000; Manchester, 2001). Nevertheless, eIF2B has been shown to form stable foci *in vivo*, and eIF2 is thought to shuttle in and out of these foci (Campbell *et al.*, 2005). Also, a recent study has examined events downstream of 43S formation,

including mRNA recruitment, scanning and 40S subunit joining. It has been suggested that the control of translation initiation is distributed between all these steps, rather than being subject to specific bottlenecks (Sangthong *et al.*, 2007), a view that is consistent with classical metabolic control analysis (Kacser and Burns, 1973; Fell, 1997). In addition, genome-wide translational profiling has provided unprecedented quantitative perspectives of global mRNA translation (Arava *et al.*, 2003; MacKay *et al.*, 2004). Collectively, these datasets provide a strong platform for the development of a computational model of translation initiation in yeast.

The complexity of translation initiation results mainly from the intricate molecular interactions between the individual components of this apparatus. Ribosome assembly alone involves more than 20 known biomolecular interactions involving various components, whose affinities depend on the direct binding partners and the other factors to which they are bound (Kapp and Lorsch, 2004; Marintchev and Wagner, 2004). eIF3 interacts with six other eIFs as well as the small 40S ribosomal subunit. If the binding of one partner does not preclude the interaction with another, then eIF3 could in theory be involved in 127 different complexes. Such a system would be relatively intractable. Hence the complexity of our model has been reduced by making a number of assumptions, some of which may be relaxed when more kinetic data become available in the future. The complete set of equations and parameter estimations are described in the Supporting information, and the model is available in SBML format in the BioModels Database (MODEL8459127548).

eIFs 1, 2, 3 and 5 form a preinitiation complex with the 40S ribosomal subunit in a cooperative manner. The experimental evidence suggests that the ternary complex is recruited to the 40S subunit, at least in part, through a stable multifactorial complex comprising the ternary complex with eIFs 1, 3 and 5 *in vivo*, the integrity of which is crucial for translation initiation (Asano *et al.*, 2000; Singh *et al.*, 2004, 2006, 2007; Reibarkh *et al.*, 2008). To reduce the complexity of modelling partially formed preinitiation complexes on 40S, it was assumed that the ternary complex binds to the 40S subunit as part of the multifactorial complex. eIF1A binds directly to the 40S subunit, promoting an open conformation that is capable

of accepting other eIFs and is scanning-competent. The thermodynamic coupling between the binding of eIF1 and eIF1A to 40S is thought to ensure that the 40S subunit is saturated with eIF1A once eIF1 is bound under *in vivo* conditions (Maag *et al.*, 2003; Passmore *et al.*, 2007). Hence, for the sake of simplicity, eIF1A was ignored in our model.

A further simplification relates to steps following the interaction of the mRNA with the 43S complex. This 43S complex (40S : eIF2·GTP : Met-tRNA<sub>i</sub><sup>Met</sup>), which interacts with mRNA to form a 48S·mRNA complex, subsequently recognizes the start codon. After the release of numerous eIFs, the 60S subunit joins the preinitiation complex with the help of eIF5B·GTP and eIF1A. However, our long-term interests relate to amino acid starvation (You *et al.*, 2007) and these steps are not subject to regulation under these conditions (Hinnebusch, 2005), i.e. they are not thought to contribute to the kinetic behaviour of the system during amino acid starvation. Hence, these steps have been grouped together in the first-order reaction  $v_{33}$  (Figure 2).

Levels of the charged initiator Met-tRNA<sub>i</sub><sup>Met</sup> and the large 60S ribosomal subunit were considered constant and were absorbed into  $k_{14}$  and  $k_{33}$ , respectively. The total number of accessible mRNA molecules was also assumed to be constant. The loading of a new 40S ribosomal subunit onto an mRNA may be affected by steric hindrance caused by subunits and ribosomes that are already associated with this particular mRNA. To address this,  $k_{32}$  was defined as a parameter that relates to the number of translating ribosomes (Skjøndal-Bar and Morris, 2007). In addition, the overall rate of mRNA translation was assumed to be directly proportional to the concentration of charged tRNAs and the number of translating ribosomes. The translation rate was assumed to be uniform along the mRNA at 10 codons/s ( $k_{33}$ ) (Arava *et al.*, 2003).

The molecular abundances of all components in the system were either taken from the literature, or estimated from reported concentrations by assuming an average cellular volume of 29 nm<sup>3</sup> (Hans *et al.*, 2003; Arava *et al.*, 2003; Singh *et al.*, 2007). Some kinetic parameters were obtained from the literature, or estimated based on published data (Arava *et al.*, 2003; Guth *et al.*, 2005; Rosen *et al.*, 2006). The remaining parameters were optimized against intermediate complex levels observed for

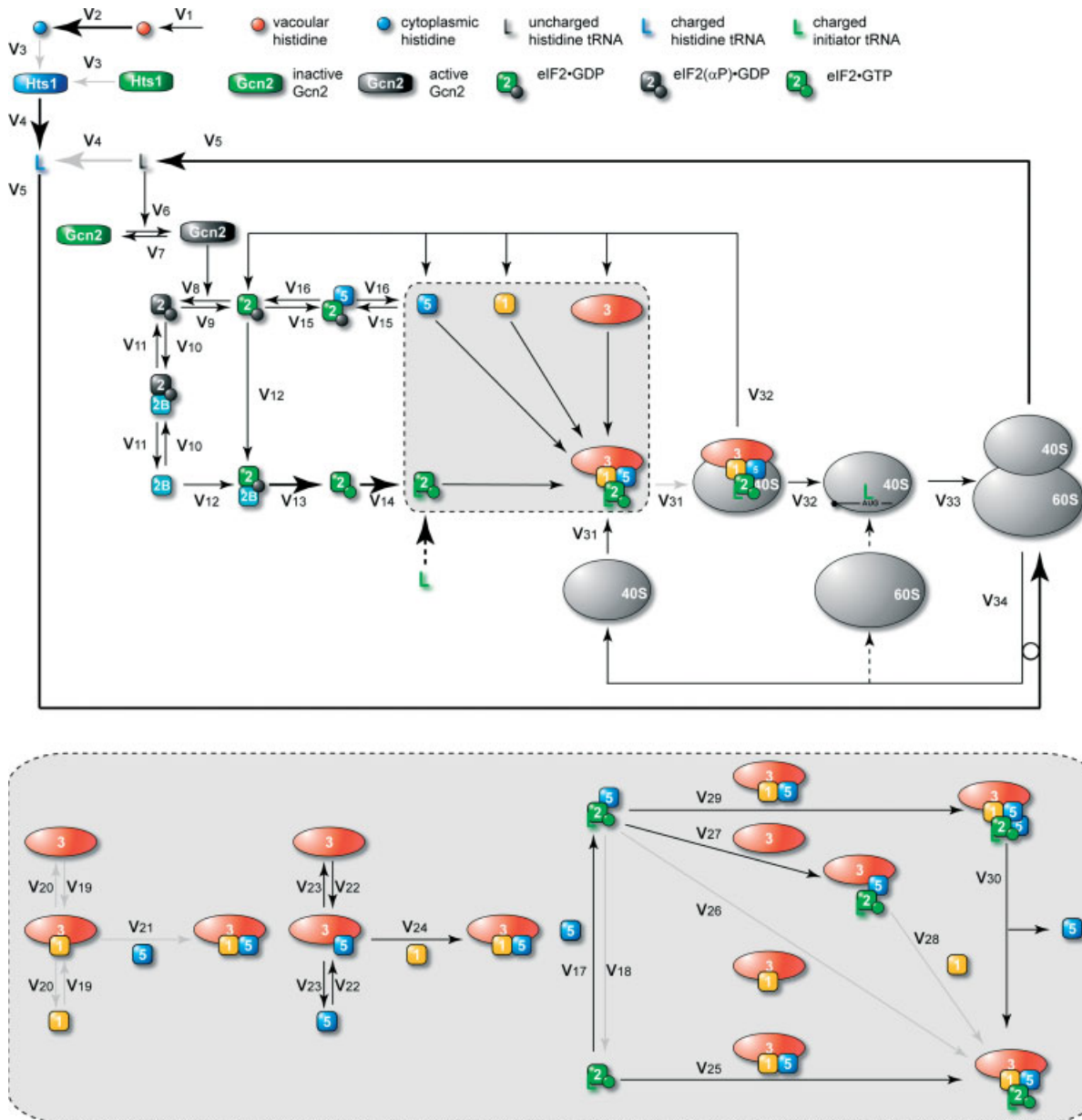


**Figure 2.** The reaction network model. Each arrow denotes a reaction. Those in grey are low-sensitivity reactions whose kinetic parameters could not be predicted accurately by the experimental data. Large arrowheads indicate reactions that significantly affect translation rates (for details, see Supporting information, sections 2.1 and 2.2). Dotted arrows denote the reactions considered implicitly in the model. The circle linking reactions  $v_5$  and  $v_{34}$  reflects the dependence of  $v_5$  upon  $v_{34}$

yeast cells grown in rich YPD medium (Singh *et al.*, 2007) by searching the physiologically relevant parametric space, using an evolutionary computing algorithm (Runarsson and Yao, 2005; see Section 1.4 of the Supporting information for an example of how we defined the physiologically

relevant parametric space). Due to the high dimensionality of the network, it is impossible to constrain all unknown kinetic parameter values. In this case, it is important to evaluate the importance of the exact values of the individual parameters. To this end, we analysed the impact of each



parameter (reported values, values calculated based on reported values, and unknown values) upon model fitness to the experimental data that were used to constrain unknown parameters. We found that the model fitness was indeed sensitive to the majority of the parameters (see Supporting information, Figure S4). However, it was also important to evaluate the impact of insensitive kinetic parameters (Figure 2; grey arrows). Therefore, a simple sensitivity analysis was carried out to investigate each parameter's impact upon the system output  $v_{34}$ . We found that the insensitive parameters previously found from model fitness sensitivity analyses either did not significantly impact upon  $v_{34}$ , or had been obtained from the literature (reported values or calculated based on reported values) (Figure 2; see also Supporting information, grey arrows in Figure S5). We conclude that the model's prediction regarding system output  $v_{34}$  is reliable, and that the kinetic parameters are reasonably parameterized. The model was next used to delineate the operational status of the translation machinery of an average *S. cerevisiae* cell growing in YPD medium.

### The impact of eIF levels upon translation rate

Translation initiation comprises several well-characterized steps in which each initiation factor is thought to play a distinct role (Figure 1). For example, eIF2 is involved in start codon selection. In contrast, eIF3 enhances ternary complex recruitment by stabilizing other eIFs on the 40S subunit, and mutations that impair eIF3 activity suppress mRNA translation (Valášek *et al.*, 2004; Maag *et al.*, 2005). Recent work suggests that in the scanning ribosomal complex, eIF2·GTP, is in equilibrium with eIF2·GDP·Pi before the complex encounters the start codon. This equilibrium is catalysed by eIF5, whilst eIF1 prevents premature release of the phosphate moiety. Upon recognition of the start codon, the pre-initiation complex undergoes a conformational change that leads to eIF1 release. This triggers subsequent release of eIF2·GDP and eIF5 and allows the 40S subunit to bind eIF5B·GTP, thereby promoting the interaction of the 60S subunit (Cheung *et al.*, 2007). Therefore, eIF1 and eIF5 play crucial roles in controlling translation initiation. The removal of eIF1 abolishes the accuracy of start codon selection, whereas dysfunctional eIF5 impairs the

ability of the preinitiation complex to initiate translation (Asano and Sachs, 2007). Therefore, intuitively one might predict that reducing the levels of either eIF1 or eIF5 would significantly decrease translational activity. We have tested the impact of perturbing the levels of individual eIFs upon translation *in silico*. Our model predicts that the rate of mRNA translation ( $v_{34}$ ) is most sensitive to reductions in eIF2. This can be explained by the fact that decreases in eIF2 activity lead to a reduction in ternary complex levels, which consequently lowers the formation of the multifactorial complex. The model's prediction that regulating eIF2 is the most efficient way of controlling the rate of mRNA translation is consistent with the observation that eIF2 has been shown experimentally to be an important control point *in vivo* (Hinnebusch, 2005). The model predicts that translation is less sensitive to changes in eIF1 and eIF5 activity (Figure 3). In fact, according to the model, the rate of translation would remain unaffected even following a five-fold reduction in each of these factors, suggesting that translation initiation is relatively robust.

Although eIFs form an equimolar multifactorial complex to initiate translation, they are not present in equal amounts in the cell (von der Haar and McCarthy, 2002; Ghaemmaghani *et al.*, 2003; Singh *et al.*, 2007). Of the eIFs 1, 2, 3 and 5, eIF3 is the least abundant in the cell,

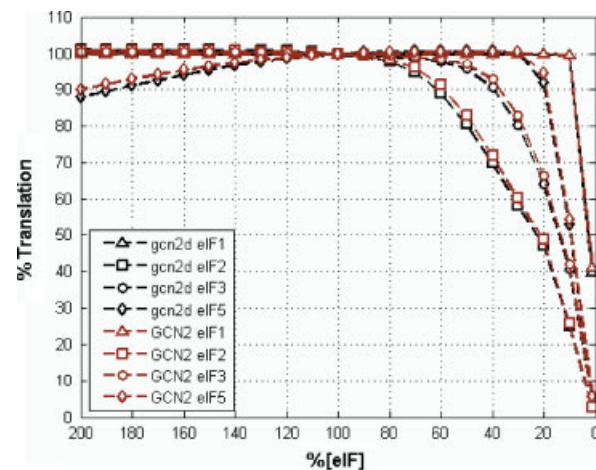


**Figure 3.** The impact of eIF levels upon mRNA translation ( $v_{34}$ ). The levels of eIFs 1, 2, 3 and 5 varied in the range 1–200% of normal levels in wild-type (*GCN2*) and *gcn2Δ* cells. The relative rate of translation (%) was normalized to the translation rate in *gcn2Δ* cells without perturbation

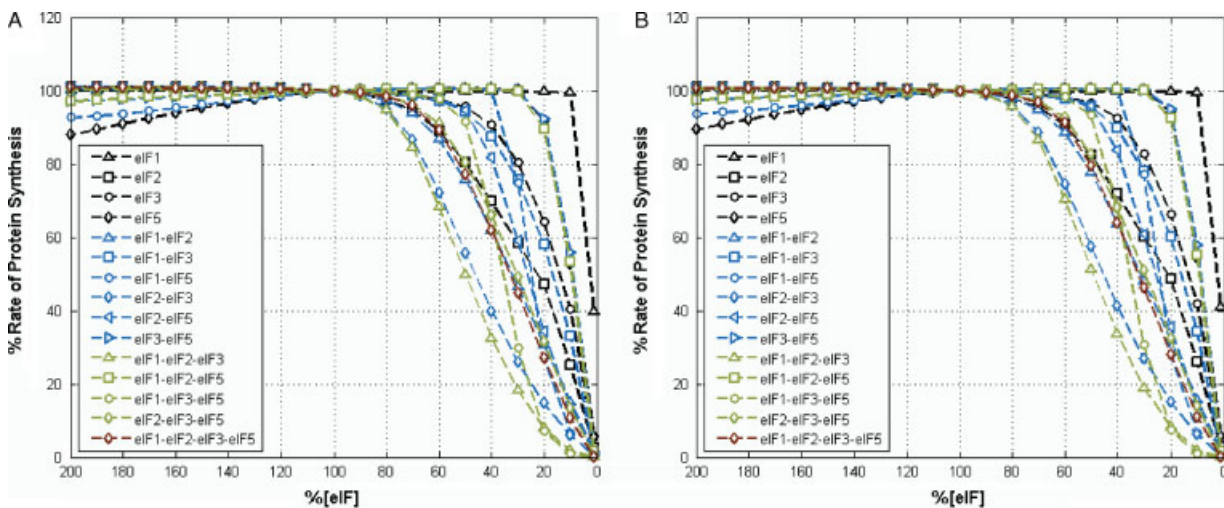


**Figure 4.** Impact of simultaneous decreases in eIF abundance upon mRNA translation in *gcn2Δ* (A) and wild-type cells (B). Rates of translation were normalized against those for each strain without perturbation

with about 33 000 copies/cell. The abundances of eIF2 and eIF5 are roughly two-fold greater than eIF3, while eIF1 is about 2.5-fold more abundant than eIF3 (Singh *et al.*, 2007). Hence, we studied the impact of relative amounts of eIFs on translation using the model. First, we examined the impact of increasing individual eIF levels upon translation. This did not enhance translation (Figure 3). In agreement with the above finding, elevating eIF5 reduced translation because this is predicted to stabilize the eIF2–eIF5 complex (by mass action), thereby suppressing eIF2B binding and GDP–GTP exchange on eIF2 (Singh *et al.*, 2006). We then tested whether the inactivation of the eIF2 $\alpha$  kinase, Gcn2, is likely to alter the effects of modulating eIF levels upon translational activity. Our model predicts that translational activity is as responsive to eIF levels in *gcn2* as wild-type cells (Figure 3).

These findings encouraged us to explore the effects of simultaneous changes in different eIFs upon translation rates. Due to the intricacy of the initiation pathway, our intuition often fails to predict the effects in complex scenarios. For example, decreasing eIF5 impedes translation initiation by limiting the formation of the multifactorial complex. On the other hand, a reduction in eIF5 also destabilizes the eIF2–eIF5 complex, favouring translation. Hence, it is difficult to predict how decreases in eIF5 would affect translation initiation when other eIFs are also

reduced. The simulation results of our model suggest that reducing the levels of a factor other than eIF5 in combination with eIF2 further inhibits translation compared to reducing eIF2 alone (in Figure 4, cf. ‘eIF1–eIF2’, ‘eIF2–eIF3’ and ‘eIF1–eIF2–eIF3’ with ‘eIF2’.) However, decreasing eIF5 levels at the same time is predicted, paradoxically, to increase translation (in Figure 4, cf. ‘eIF1–eIF2’ with ‘eIF1–eIF2–eIF5’, ‘eIF2–eIF3’ with ‘eIF2–eIF3–eIF5’ and ‘eIF1–eIF2–eIF3’ with ‘eIF1–eIF2–eIF3–eIF5’, respectively.) Once again, Gcn2 inactivation was predicted to have a minimal effect upon the impact of modulating eIF levels upon translational activity (Figure 4).

Our data suggest that simultaneous decreases in multiple factors do not necessarily inhibit translation more strongly than decreasing the corresponding initiation factors singly. Our attempts to maximize the translation rate by simultaneously changing the levels of the four eIFs within a 10-fold range of their normal *in vivo* abundances failed to define an alternative combination of abundances that yielded higher translation rates. The results of these simulations suggest that eIF levels in yeast have evolved such that translation rates are optimized during growth on rich media, such as YPD. This suggests that the presence of sufficient amounts of eIFs, rather than equimolar amounts of eIFs, ensure the highest translation activity. It also illustrates the importance of a systems approach to understanding complex biological processes.



### Analysis of translation robustness against eIF1 variation

In the previous section, relative mRNA translation activity was used as a measure of the robustness of the translational initiation apparatus. In particular, we regarded experimentally determined molecular abundances with the corresponding set of kinetic parameter values as the nominal condition, and analysed the 'percentage translation' at different eIF1 levels in comparison with the nominal condition. This was a useful starting point for discussion. However, biological robustness represents the maintenance of a specific biological function following exposure to a range of internal and external perturbations. Therefore, to characterize the robustness of a system, we must define relevant internal and external perturbations. Internal perturbations may be exerted as noise in molecular abundance and kinetic parameter values, while external perturbations can be exerted through inputs to the system. In this case there is a single input, amino acid (histidine) uptake rate ( $v_1$ ). Hence, we investigated how the output of this system (the mRNA translation rate,  $v_{34}$ ) responded to internal and external perturbations.

First, we investigated how noise in molecular abundance and kinetic parameter values affected relative rates of translation at different levels of eIF1. The abundance of eIFs was found to vary *in vivo* by about 20% (Ghaemmaghami *et al.*, 2003; Singh *et al.*, 2007). For this reason the molecular abundances and kinetic parameter values in our model were assumed to conform to Gaussian distributions, with nominal values as the means and standard deviations (SDs) of 20% of the means. 5000 wild-type cells were randomly generated and simulated, and the steady-state mRNA translation rates calculated for each cell. The SD of the steady-state mRNA translation rate for the population as a whole was about 30% of the mean value. This is consistent with published experimental data on the observed variation in expression capacity of *S. cerevisiae* cells (Colman-Lerner *et al.*, 2005).

For each cell, the relative translation rate at 10% of the normal eIF1 level was calculated by comparing its translation at 10% eIF1 with the original value (Figure 5A, upper inset). Here, we used total parameter variation to represent the total parametric deviation of a cell from the nominal condition. Its definition is given by equation (1), where  $s_o^i$

and  $k_o^j$  are the nominal values for the molecular abundance of species  $i$  and the kinetic parameter  $j$ , respectively, while  $s^i$  and  $k^j$  are their values for the cell (Barkai and Leibler, 1997). The lower this numerical value (it is always  $>1$ ), the more closely the cell resembles the nominal condition, and vice versa. For cells with lower than a certain total parameter variation ( $10^3$ ,  $10^4$ ,  $10^5$  and  $10^6$ ), we calculated the fraction of the cells with  $>90\%$  relative translation rates. This was defined as the cumulative fraction at that total parameter variation. The cumulative fractions were plotted against total parameter variations. Strikingly, this plot illustrates that the high relative translation rate does not change across a wide range of total parameter variations (Figure 5A, lower inset). Significantly, nearly 90% of all cells display  $>90\%$  translation, even when total parameter variation is as high as  $10^6$ . This suggests that translation initiation in individual cells may not be significantly affected by variations in molecular abundances and kinetic parameters across a wide range of eIF1 levels:

*Total parameter variation*

$$= \exp \left( \sum_{i=1}^m \left| \log \frac{s^i}{s_o^i} \right| + \sum_{j=1}^n \left| \log \frac{k^j}{k_o^j} \right| \right) \quad (1)$$

It is worth noting that robustness is a property that belongs to an individual network. Hence the collective behaviour of a cohort of robust individuals may not be robust. To test this, the above data were normalized against the average translation rate at 100% eIF1 for the entire population (Figure 5B, upper inset). The results exhibited a coefficient of variation that was 20% higher than the previous case [in Table 1, cf.  $\sigma/\mu$  for (A) and (B)]. This relatively large dispersion results in the fact that  $<60\%$  of all cells possess  $>90\%$  relative translation rate at 10% eIF1 (Figure 5B, lower inset). This population heterogeneity would probably mask the robustness exhibited by individual cells. In fact, it raises questions about the validity of comparing the translation rates for cell populations at 10% and 100% eIF1 levels, given the large variations inherent within individual populations (Figure 5C, D).

In most biochemical or genomic experiments, we measure and compare the mean of the means of the collective behaviour of a cell population and

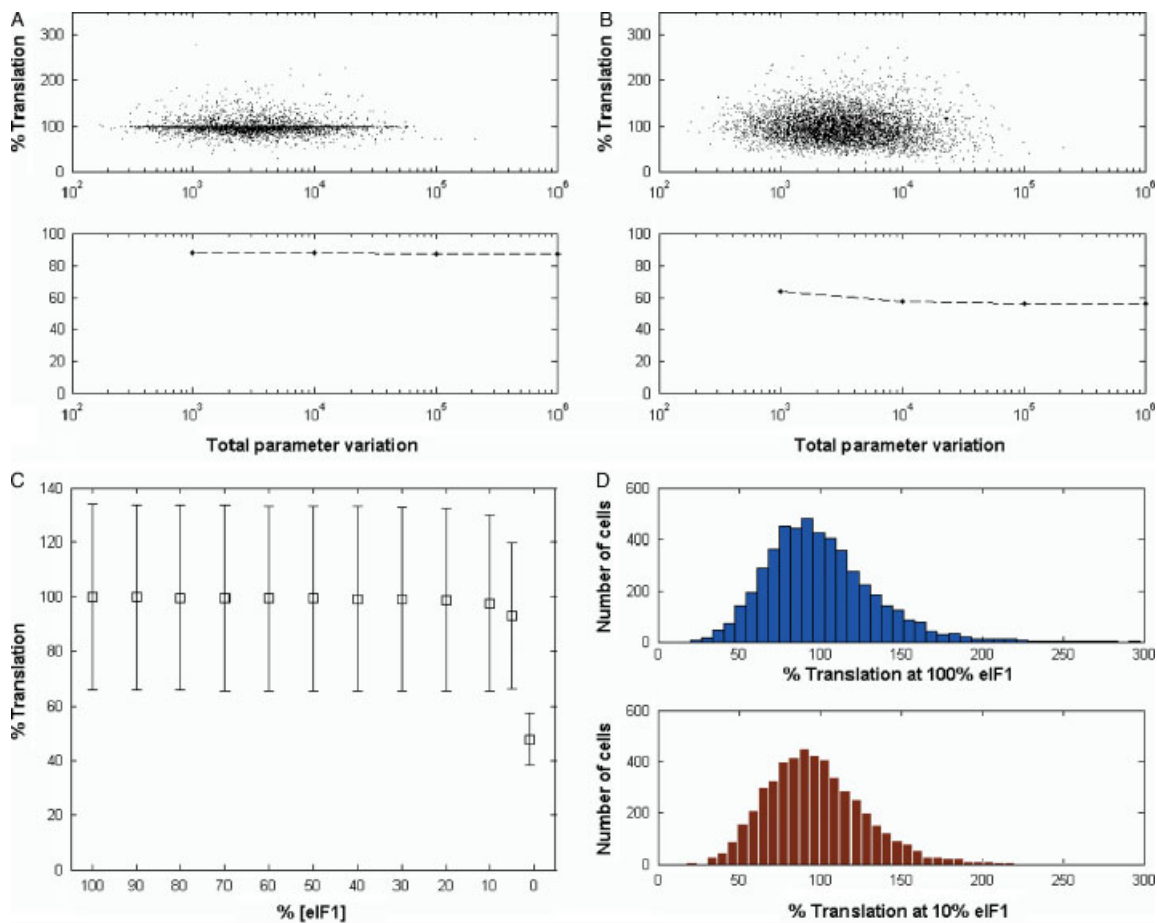


**Figure 5.** Effect of at eIF1 level upon translation rates in 5000 randomly generated cells. To generate each cell, the abundance of individual molecular species and kinetic parameter values were assumed to conform to Gaussian distributions, with nominal values as the means, and SDs of 20% of the means. Relative translation at 10% eIF1 for each cell is normalized against either its own translation rate at 100% eIF1 (A), or the average translation rate at 100% eIF1 for the entire population (B). In (A) and (B), the upper plots show the effects of 10% eIF1 translation percentage against total parameter variation. The lower plots present the cumulative fraction of >90% translation percentage against total parameter variation. (C) Translation at different eIF1 levels. Note that eIF1 is essential for viability, and that the lowest eIF1 level tested was 1% of nominal values. The model predicts zero translation when eIF1 is absent. (D) Histogram of translation percentages at 10% and 100% eIF1. Data in (C, D) were normalized against the average translation rate at 100% eIF1 for the entire population

**Table 1.** Statistics for the cell population in Figure 5

	Mean ( $\mu$ )	Standard deviation ( $\sigma$ )	Coefficient of variation ( $\sigma/\mu$ )	Correlation coefficient $\rho_{\%translation,TPV}$
A	98.8%	13.1%	0.133	0.0526
B	97.8%	32.1%	0.328	0.0914

often draw conclusions regarding the behaviour of individual cells. For example, the expression of eIF1 could be modulated by placing its gene

under the control of a tetracycline-responsive promoter. Then, under each experimental condition, one could measure the average translational status of millions of cells a number of times, and regard the average of these mean values as the representative value of the translational status at a particular eIF1 level. Further measurements of such means of means could then be obtained for additional experimental conditions, and conclusions drawn by comparing these results. To illustrate this, we randomly divided the 5000 cells into five groups of 1000

cells. We calculated the average translation rate for each group at 10% and 100% eIF1 levels and calculated the mean of the means. In fact, the five *in silico* measurements were highly reproducible (with <1% coefficient of variations). Although the mean of the mean values were similar (10% eIF1, 5490 proteins/s; 100% eIF1, 5614 proteins/s), a *t*-test rejects the null hypothesis that the mean of the average translation rates are the same at the 5% significance level. Let us assume that the quality and quantity of experimental measurements of eIF levels and other molecular components are sufficiently high, i.e. that the experimental error and intrinsic noise do not render our biological comparisons meaningless. Then, in principle, we would be able to produce some highly reproducible data (around 1% coefficient of variation) and compare the mean of the average translation rates at 10% and 100% eIF1. However, before doing this, we should ask whether it is meaningful to compare data in this way, since these data exhibited a high degree of variation. In other words, we could not exclude the albeit unlikely possibility that there might be a significant fraction of cells that display significantly higher translation rates when eIF1 is reduced, but that the effect of this fraction is offset by another fraction of cells that display significantly lower translation rates at reduced eIF1 levels. Hence, in practice, our observations relating to translational activity at the two eIF1 levels may be inconclusive because of inherent noise in the experimental data (approximately 30% coefficient of variation; Table 1). This highlights the inherent danger in evaluating the system properties of individual cells based on measurements of cell populations, and suggests the importance of single-cell experiments when dealing with cellular properties that may not be obvious at the population level (Colman-Lerner *et al.*, 2005).

We then performed similar analyses for other eIFs. We found that translation activity is not significantly affected, even following a five-fold reduction in eIF5. However, the translation rate was predicted to be more dependent on the levels of eIF2 and eIF3 (see Supporting information, Section 3, Robustness analysis).

In summary, our model predicts that the rate of mRNA translation initiation in individual yeast cells is not significantly affected by wide-ranging variations in eIF1 levels. The model also predicts

that this property is obscured by population heterogeneity in mRNA translation rates from cell to cell.

### Robustness against an external perturbation

Next we investigated the impact of external perturbation upon the rate of mRNA translation by simulating the effects of varying the rate of histidine uptake (the single input to the system; Figure 2). This was done using the same cell population that was used to analyse the effects of internal perturbations (discussed above). The steady-state rate of histidine uptake was calculated for each of these 5000 cells. This value was then lowered to a particular percentage of its original value (e.g. 90%, 20%, 10%, 5% or 1%) to simulate the effects of histidine starvation upon the rate of mRNA translation. In contrast to the observed robustness of this system to changing eIF1 levels, the relative translation rate decreases significantly when the rate of histidine uptake was lowered (Figure 6A). For example, lowering the histidine uptake rate to 20% of the original value for each individual cell led to about a four-fold decrease in translation rate (Figure 6B). This prediction is consistent with the experimental observation that the guanine nucleotide exchange activity of eIF2B is four-fold lower when histidine starvation is imposed using the histidine analogue 3-aminotriazole (3AT: Campbell *et al.*, 2005). The prediction is also consistent with the observation that yeast translation rates are reduced during amino acid limitation (Hinnebusch, 2005).

The sensitive response to amino acid availabilities should come as no surprise, as this is consistent with the functionality of the network. In other words, the regulation of general mRNA translation by *Gcn2* is maintained in the face of certain degree of variation in *Gcn2* activity, defined by the values of  $k_6$ ,  $k_7$ ,  $k_8$  and  $k_9$ . This also demonstrates the robustness of the workings of this regulatory mechanism.

### Possible regulatory mechanisms under amino acid starvation

We have also used the model to investigate the changes in the eIF factors and partially formed complexes on the initiation pathway under different amino acid availabilities. The model suggests

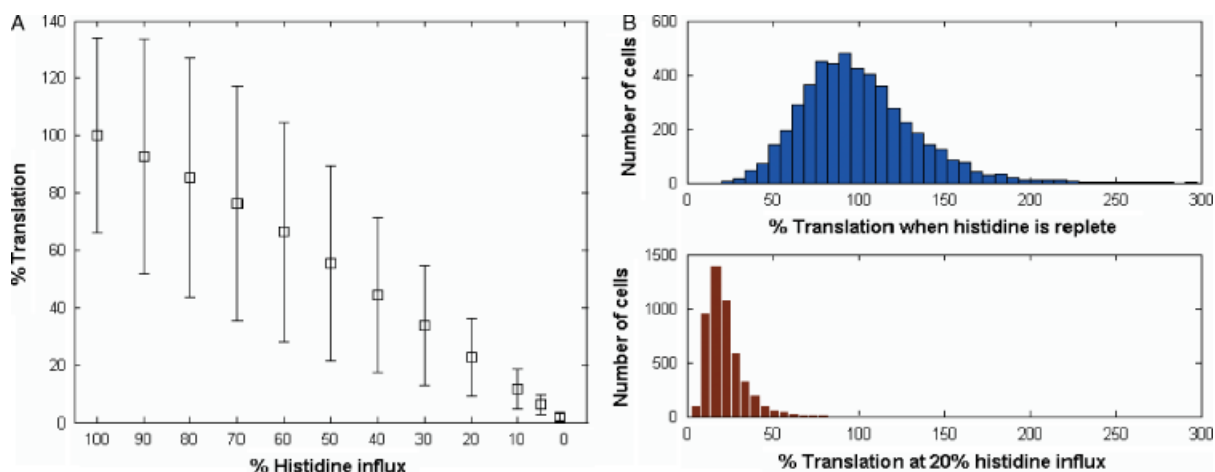


**Figure 6.** Impact of histidine uptake rate upon translational activity. The same cell populations were used as for Figure 5. Relative translational activity at different histidine uptake rates for each cell is normalized against the average translation rate at 100% uptake of the entire population. (A) Translation at different histidine uptake rates. (B) Histogram of translation percentages at 20% and 100% histidine uptake rate

that the level of the eIF1–eIF3–eIF5 complex significantly increases under amino acid starvation conditions (i.e. low  $v_1$  levels). This increase is consistent with the hypothesis that an unidentified factor regulating start codon recognition is upregulated when amino acids become limiting and hence positively modulates the translation of *GCN4* mRNA ('Factor X' in Grant *et al.*, 1994). This finding suggests a possible regulatory role of the eIF1–eIF3–eIF5 complex and merits further experimental investigation.

## Discussion

We have developed a quantitative model that describes mRNA translation in yeast cells growing in rich YPD medium. We have developed this model by integrating diverse datasets from the literature. These data include *in vitro* assays of the dissociation constants for interactions among molecular components involved in translation initiation (Maag *et al.*, 2003, 2005; Singh *et al.*, 2004, 2007), kinase activities involved in aminoacylation (Rosen *et al.*, 2006), *in vivo* measurements of the intermediate complex levels on the translation initiation pathway (Campbell *et al.*, 2005; Singh *et al.*, 2007) and genome-wide polysome profiling datasets (Arava *et al.*, 2003). We have used this model to predict the effects of internal and external perturbations upon mRNA translation rates. Our

main finding is that, under these growth conditions, yeast mRNA translation appears to be remarkably robust in the face of internal perturbations and yet remains responsive to external perturbations, such as amino acid limitation. A number of other interesting predictions have arisen from the model.

First, contrary to our intuitive expectation, the model predicts that translation initiation is relatively insensitive to wide-ranging variations in the levels of eIF1 and eIF5. This prediction is consistent with a recent study that surveyed the effects of depleting eIF2, eIF3 and eIF5 upon translation (Jivotovskaya *et al.*, 2006). These authors showed that translation is more robust to reductions in eIF5 levels than to reductions in eIF2 or eIF3. The dramatic depletion of eIF2 or eIF3 alone resulted in a large reduction in polysomes and the accumulation of 80S monosomes, whereas the depletion of eIF5 elicited a less dramatic decrease in cellular polysome content (Jivotovskaya *et al.*, 2006). This is entirely consistent with our predictions (Figure 3). Indeed, a peak of halfmer (representing a 48S initiating at the 5' UTR and an elongating 80S) is present when eIF5 is depleted, but is absent following eIF2 or eIF3 depletion (Jivotovskaya *et al.*, 2006). In addition, this halfmer peak is still present when eIF2 and eIF5 (or eIF3 and eIF5) are simultaneously depleted (Jivotovskaya *et al.*, 2006). This suggests that a simultaneous decrease in eIF2 and eIF5 (or eIF3 and eIF5) might have a less severe effect upon translation reduction than a

reduction in eIF2 (or eIF3) alone. Again, this is in agreement with the predictions of our model.

eIF1 is thought to bind directly to the 40S subunit with high affinity ( $16 \pm 2$  nM in the absence of eIF1A, and  $6.1 \pm 0.8$  nM in the presence of eIF1A; Maag and Lorsch, 2003). In addition, most eIF1 molecules are not associated with complexes containing other eIFs in yeast cells growing on YPD (Singh *et al.*, 2007). Even without the stabilizing effects of other initiation factors, the abundance of eIF1 (about 81 000 molecules/cell) would saturate unengaged 40S subunits (approximately 20 000/cell, assuming that 90% of the 200 000 ribosomes in the cell are engaged in translation during growth in YPD; Singh *et al.*, 2007). This suggests that eIF1 is in excess under these growth conditions. Therefore, it is reasonable that even a 10-fold reduction in eIF1 levels would exert minimal effects on mRNA translation rates (Figures 3, 5). This can also be explained in terms of the critical functionality of eIF1. The high levels of this critical component might buffer individual cells against the potentially severe phenotypes that could arise from the high translational error rates that result from erroneous codon–anticodon selection in the absence of sufficient eIF1.

In principle, eIF1 activity can be lowered by decreasing the levels of this factor or by mutations that render eIF1 dysfunctional, such that it cannot bind 40S subunit or other eIFs. However, eIF1 mutations are likely to have more profound impacts upon mRNA translation. For example, eIF1 mutations substantially lower the affinity of eIF1 for 40S, thereby significantly impairing the stringency of start codon selection (Cheung *et al.*, 2007). This can be explained by incorporating two additional reactions in the current model: a reverse reaction that counteracts reaction  $v_{31}$ , and a reaction that describes the premature release of eIF1 during scanning (data not shown). Therefore, lowering the levels of wild-type eIF1 should not be confused with impairing eIF1 functionality through genetic insults. Hence our observation that mRNA translation is relatively insensitive to the lowering of eIF1 levels is not inconsistent with the observed phenotypic impact of eIF1 mutations.

The second prediction of the model is that yeast mRNA translation rates decline significantly following histidine starvation (Figure 6). Together with the previous point, our observations indicate that, while yeast mRNA translation is robust

when exposed to internal perturbations, it remains responsive to external perturbations. However, our simulations of cell populations suggests that this robustness is a property of individual cells and might not be reflected in the behaviour of the entire population. This also questions the adequacy of population-based experiments in evaluating the properties of individual cells.

To investigate translational robustness, we assumed 20% coefficient variation for all components in the network and kinetic parameters. However, a recent report has suggested that the noise in translation initiation factor protein levels might be slightly lower than this (Newman *et al.*, 2006). In addition, we used Gaussian distribution to mimic protein fluctuations, by implicitly assuming that the noise in protein levels is dominated by protein production and degradation, and that such a Poisson distribution can be approximated by Gaussian distribution. However, it is known that noise in gene activation–inactivation and spontaneous ‘birth and death’ of mRNA can make protein fluctuations deviate from the Poisson distribution (Paulsson, 2005). Indeed, recent independent genome-wide assays into protein noise confirmed this deviation (Bar-Even *et al.*, 2006; Lu *et al.*, 2007). However, the purpose of our study was to investigate the changes in translation activity in response to internal and external perturbations, given the parameter and initial condition fluctuations. Therefore, we neglected these differences and used Gaussian distribution as an approximation. In addition, our survey did not intend to capture the internal noise elicited by stochastic chemical reactions. Hence, we used the ODE system to evaluate the impacts of these perturbations.

In the design of any biological system, there is a trade-off between robustness and performance (Kitano, 2007). In our case, the presence of Gcn2 enhances the robustness of mRNA translation to variations in eIF levels (Figure 3; cf. *gcn2*Δ with wild-type strains). This effect can be magnified by altering the binding affinity of Gcn2 for uncharged tRNA and the eIF2α kinase activity of Gcn2 simultaneously (Figure 7). Enhancing the binding affinity for uncharged tRNA is predicted to enhance the sensitivity of Gcn2 regulation; whilst elevating its catalytic activity is predicted to have a similar effect. Increasing either of these properties is predicted to make translation less sensitive to decreased eIF1 levels, while



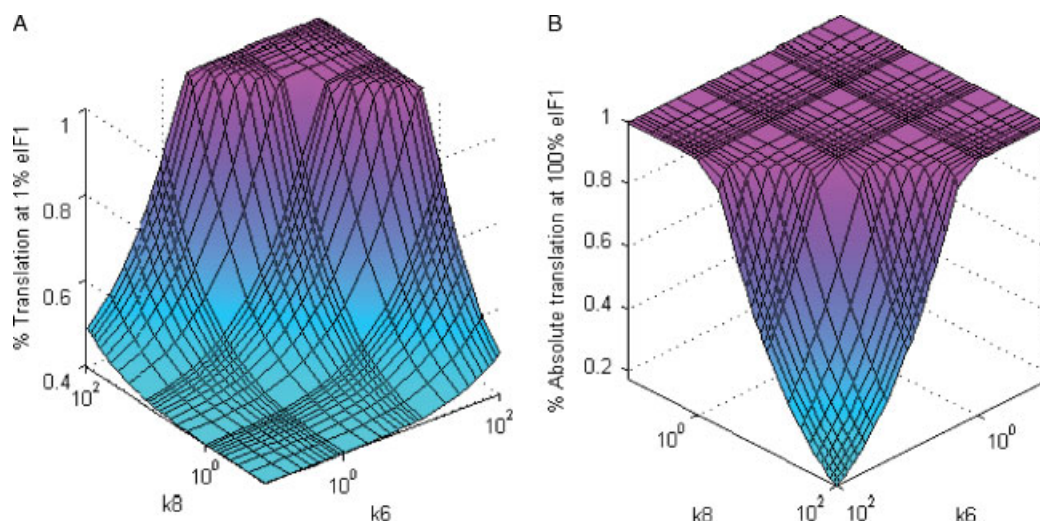


**Figure 7.** The trade-off between robustness and performance in yeast mRNA translation. (A) Percentage of translation at 1% eIF1 when Gcn2 assumes different binding affinities to uncharged tRNAs ( $k_6$ ) and kinase activities ( $k_8$ ) (0.01–10-fold changes of the nominal values, normalized against corresponding translation rate at 100% eIF1). (B) Percentage of absolute translation at 100% eIF1 at different  $k_6$  and  $k_8$  values (normalized against translation rate under the nominal condition).  $k_6$  and  $k_8$  axes are in reverse order

the actual rate of mRNA translation is decreased (Figure 7). This exemplifies the trade-off in the robustness and performance of the mRNA translation apparatus.

Histidine starvation has been addressed in this model (as opposed to the starvation of other amino acids) primarily because the bulk of the published experimental data address histidine starvation in yeast (for review, see Hinnebusch, 2005). In principle, our model can describe the combinatorial starvation of any amino acids, as long as the experimental data were available to estimate the corresponding molecular abundance and kinetic parameters. In addition, our model could be extended to describe the kinetics of rapamycin-induced global translation arrest in yeast by linking our model with an existing model of the TOR signalling pathway (Kuepfer *et al.*, 2007), e.g. through TOR signalling to Gcn2 and eIF4E. Therefore, we regard the framework presented here as a starting point for the modelling and simulation of the Gcn2-mediated control of mRNA translation.

### Acknowledgements

We thank Dr Ian Stansfield (University of Aberdeen), Professor Katsura Asano (Kansas State University) and Professor Daniel Herschlag (Stanford University) for their

valuable discussions and suggestions. We are very grateful to Dr Yoav Arava (Israel Institute of Technology) for insightful discussions on estimating the number of translating ribosomes and sharing his global mRNA translational profiling data. T.Y. gratefully acknowledges the support of a 6th Century Studentship (University of Aberdeen) and an ORSAS studentship. T.Y., G.M.C. and A.B. are supported by the BBSRC (BB/F00513X/1) under the Systems Approaches to Biological Research (SABR) initiative.

### Supporting information on the internet

The following supporting information is to be found in the online version of this article:

A quantitative model for mRNA translation in *Saccharomyces cerevisiae*:

1. Model construction
  - 1.1. Biochemical formulation of the model
  - 1.2. Mathematical formulation of the model
  - 1.3. Molecular abundance
  - 1.4. Kinetic parameter estimation
2. Model validation
  - 2.1. Sensitivity analysis of the kinetic parameters
  - 2.2. Kinetic parameter's impact on translation rate
3. Robustness analysis
  - 3.1. Robustness of general translation against variations in eIFs 2,3

### 3.2 Robustness of general translation against variations in eIF5

#### References

Figures S1–S7

Tables S1–S7

#### References

- Acker MG, Shin BS, Dever TE, Lorsch JR. 2006. Interaction between eukaryotic initiation factors 1A and 5B is required for efficient ribosomal subunit joining. *J Biol Chem* **281**(13): 8469–8475.
- Algire MA, Maag D, Savio P, *et al.* 2002. Development and characterization of a reconstituted yeast translation initiation system. *RNA* **8**(3): 382–397.
- Arava Y, Boas FE, Brown PO, Herschlag D. 2005. Dissecting eukaryotic translation and its control by ribosome density mapping. *Nucleic Acids Res* **33**(8): 2421–2432.
- Arava Y, Wang Y, Storey JD, *et al.* 2003. Genome-wide analysis of mRNA translation profiles in *Saccharomyces cerevisiae*. *Proc Natl Acad Sci USA* **100**(7): 3889–3894.
- Asano K, Clayton J, Shalev A, Hinnebusch AG. 2000. A multifactor complex of eukaryotic initiation factors, eIF1, eIF2, eIF3, eIF5, and initiator tRNA-Met is an important translation initiation intermediate *in vivo*. *Genes Dev* **14**(19): 2534–2546.
- Asano K, Sachs MS. 2007. Translation factor control of ribosome conformation during start codon selection. *Genes Dev* **21**: 1280–1287.
- Bar-Even A, Paulsson J, Maheshri N, *et al.* 2006. Noise in protein expression scales with natural protein abundance. *Nat Genet* **38**(6): 636–643.
- Barkai N, Leibler S. 1997. Robustness in simple biochemical networks. *Nature* **387**(6636): 913–917.
- Bergmann JE, Lodish HF. 1979. A kinetic model of protein synthesis. *J Biol Chem* **254**(23): 11927–11937.
- Brockmann R, Beyer A, Heinisch JJ, Wilhelm T. 2007. Posttranscriptional expression regulation: what determines translation rates? *PLoS Comp Biol* **3**(3): e57.
- Campbell SG, Hoyle NP, Ashe MP. 2005. Dynamic cycling of eIF2 through a large eIF2B-containing cytoplasmic body: implications for translation control. *J Cell Biol* **170**(6): 925–934.
- Cherkasova VA, Hinnebusch AG. 2003. Translational control by TOR and TAP42 through dephosphorylation of eIF2 $\alpha$  kinase GCN2. *Genes Dev* **17**(7): 859–872.
- Cheung Y-N, Maag D, Mitchell SF, *et al.* 2007. Dissociation of eIF1 from the 40S ribosomal subunit is a key step in start codon selection *in vivo*. *Genes Dev* **21**: 1217–1230.
- Colman-Lerner A, Gordon A, Serra E, *et al.* 2005. Regulated cell-to-cell variation in a cell-fate decision system. *Nature* **437**(29): 699–706.
- Delbecq P, Werner M, Feller A, *et al.* 1994. A segment of mRNA encoding the leader peptide of the *CPA1* gene confers repression by arginine on a heterologous yeast gene transcript. *Mol Cell Biol* **14**: 2378–2390.
- Dholakia JN, Wahba AJ. 1989. Mechanism of the nucleotide exchange reaction in eukaryotic polypeptide chain initiation. Characterization of the guanine nucleotide exchange factor as a GTP-binding protein. *J Biol Chem* **264**(1): 546–550.
- Dimelow RJ, Wilkinson SJ. 2009. Control of translation initiation: a model-based analysis from limited experimental data. *J R Soc Interface* **6**(30): 51–61.
- Fell DA. 1997. *Understanding the Control of Metabolism*. Portland Press: London.
- Ghaemmaghami S, Huh WK, Bower K, *et al.* 2003. Global analysis of protein expression in yeast. *Nature* **425**(6959): 737–741.
- Godefroy-Colburn T, Thach RE. 1981. The role of mRNA competition in regulating translation. IV. Kinetic model. *J Biol Chem* **256**(22): 11762–11773.
- Grant CM, Miller PF, Hinnebusch AG. 1994. Requirements for intercistronic distance and level of eukaryotic initiation factor 2 activity in reinitiation on *GCN4* mRNA vary with the downstream cistron. *Mol Cell Biol* **14**(4): 2616–2628.
- Guth E, Connolly SH, Bovee M, Francklyn CSA. 2005. A substrate-assisted concerted mechanism for aminoacylation by a class II aminoacyl-tRNA synthetase. *Biochemistry* **44**(10): 3785–3794.
- Hans MA, Heinzle E, Wittmann C. 2003. Free intracellular amino acid pools during autonomous oscillations in *Saccharomyces cerevisiae*. *Biotechnol Bioeng* **82**(2): 143–151.
- Harley CB, Pollard JW, Stanners CP, Goldstein S. 1981. Model for messenger RNA translation during amino acid starvation applied to the calculation of protein synthetic error rates. *J Biol Chem* **256**(21): 10786–10794.
- Hinnebusch AG. 2005. Translational Regulation of *GCN4* and the general amino acid control of yeast. *Annu Rev Microbiol* **59**: 407–450.
- Ingolia NT, Ghaemmaghami S, Newman JR, Weissman JS. 2009. Genome-wide analysis *in vivo* of translation with nucleotide resolution using ribosome profiling. *Science* **324**(5924): 218–223.
- Jivotovskaya A, Valášek L, Hinnebusch AG, Nielsen KH. 2006. Eukaryotic translation initiation factor 3, eIF3, and eIF2 can promote mRNA binding to 40S subunits independently of eIF4G in yeast. *Mol Cell Biol* **26**(4): 1355–1372.
- Kacser H, Burns JA. 1973. The control of flux. *Symp Soc Exper Biol* **27**: 65–104.
- Kapp LD, Lorsch JR. 2004. The molecular mechanics of eukaryotic translation. *Annu Rev Biochem* **73**: 657–704.
- Kitano H. 2007. Towards a theory of biological robustness. *Mol Syst Biol* **3**: 137.
- Kuepfer L, Peter M, Sauer U, Stelling J. 2007. Ensemble modeling for analysis of cell signaling dynamics. *Nat Biotechnol* **25**(9): 1001–1006.
- Lu P, Vogel C, Wang R, *et al.* 2007. Absolute protein expression profiling estimates the relative contributions of transcriptional and translational regulation. *Nat Biotechnol* **25**(1): 117–124.
- MacKay VL, Li X, Flory MR, *et al.* 2004. Gene expression analyzed by high-resolution state array analysis and quantitative proteomics: response of yeast to mating pheromone. *Mol Cell Proteom* **3**(5): 478–489.
- Manchester KL. 2001. Catalysis of guanine nucleotide exchange on eIF2 by eIF2B: can it be both a substituted enzyme and a sequential mechanism? *Biochem Biophys Res Commun* **289**(3): 643–646.
- Marintchev A, Wagner G. 2004. Translation initiation: structures, mechanisms and evolution. *Q Rev Biophys* **37**(3–4): 197–284.

- Maag D, Lorsch JR. 2003. Communication between eukaryotic translation initiation factors 1 and 1A on the yeast small ribosomal subunit. *J Mol Biol* **330**: 917–924.
- Maag D, Fekete CA, Gryczynski Z, Lorsch JR. 2005. A conformational change in the eukaryotic translation preinitiation complex and release of eIF1 signal recognition of the start codon. *Mol Cell* **17**(2): 265–275.
- Newman JR, Ghaemmaghami S, Ihmels J, *et al.* 2006. Single-cell proteomic analysis of *S. cerevisiae* reveals the architecture of biological noise. *Nature* **441**(7095): 840–846.
- Nika J, Yang W, Pavitt GD, *et al.* 2000. Purification and kinetic analysis of eIF2B from *Saccharomyces cerevisiae*. *J Biol Chem* **275**(34): 26011–26017.
- Passmore LA, Schmeing TM, Maag D, *et al.* 2007. The eukaryotic translation initiation factors eIF1 and eIF1A induce an open conformation of the 40S ribosome. *Mol Cell* **26**: 41–50.
- Paulsson J. 2005. Models of stochastic gene expression. *Phys Life Rev* **2**: 157–175.
- Reibarkh M, Yamamoto Y, Singh CR, *et al.* 2008. Eukaryotic initiation factor. eIF. 1 carries two distinct eIF5-binding faces important for multifactor assembly and AUG selection. *J Biol Chem* **283**(2): 1094–1103.
- Rosen AE, Brooks BS, Guth E, *et al.* 2006. Evolutionary conservation of a functionally important backbone phosphate group critical for aminoacylation of histidine tRNAs. *RNA* **12**(7): 1315–1322.
- Rowlands AG, Panniers R, Henshaw EC. 1988. The catalytic mechanism of guanine nucleotide exchange factor action and competitive inhibition by phosphorylated eukaryotic initiation factor 2. *J Biol Chem* **263**(12): 5526–5533.
- Runarsson TP, Yao X. 2005. Search biases in constrained evolutionary optimization. *IEEE Transactions on Systems, Man, and Cybernetics* **35**(2): 233–243.
- Sangthong P, Hughes J, McCarthy JEG. 2007. Distributed control for recruitment, scanning and subunit joining steps of translation initiation. *Nucleic Acids Res* **35**(11): 3573–3580.
- Singh CR, Lee B, Udagawa T, *et al.* 2006. An eIF5/eIF2 complex antagonizes guanine nucleotide exchange by eIF2B during translation initiation. *EMBO J* **25**: 4537–4546.
- Singh CR, Udagawa T, Lee B, *et al.* 2007. Change in nutritional status modulates the abundance of critical pre-initiation intermediate complexes during translation initiation *in vivo*. *J Mol Biol* **370**: 315–330.
- Singh CR, Yamamoto Y, Asano K. 2004. Physical association of eukaryotic initiation factor, eIF, 5-carboxyl-terminal domain with the lysine-rich eIF2 $\beta$  segment strongly enhances its binding to eIF3. *J Biol Chem* **279**(48): 49644–49655.
- Skjøndal-Bar N, Morris DR. 2007. Dynamic model of the process of translation in eukaryotic cells. *Bull Math Biol* **69**: 361–393.
- Valášek L, Nielsen KH, Zhang F, *et al.* 2004. Interactions of eukaryotic translation initiation factor 3, eIF3. Subunit NIP1/c with eIF1 and eIF5 promote preinitiation complex assembly and regulate start codon selection. *Mol Cell Biol* **24**(21): 9437–9455.
- Vilela C, Linz B, Rodrigues-Pousada C, McCarthy JEG. 1998. The yeast transcription factor genes *YAP1* and *YAP2* are subject to differential control at the levels of both translation and mRNA stability. *Nucleic Acids Res* **26**: 1150–1159.
- von der Haar T, Hughes JM, Manjarul Karim M, *et al.* 2002. Translation initiation and surface plasmon resonance: new technology applied to old questions. *Biochem Soc Trans* **30**(2): 155–162.
- von der Haar T, McCarthy JEG. 2002. Intracellular translation initiation factor levels in *Saccharomyces cerevisiae* and their role in cap-complex function. *Mol Microbiol* **2**: 531–544.
- Wullschleger S, Loewith R, Hall MN. 2006. TOR signaling in growth and metabolism. *Cell* **124**(3): 471–484.
- You T, Coghill GM, Brown AJP. 2007. A Quantitative model for the translational control of *GCN4* in yeast. 2nd Foundations of Systems Biology in Engineering Conference Proceedings, Stuttgart; 121–126.